EXPLOSIVE TESTING OF CLASS 1.3 ROCKET BOOSTER PROPELLANT

Claude Merrill, Albert Nichols, and Edward Lee

ABSTRACT

Recent experimentation has provided a more thorough understanding of the explosive response of class 1.3 composite propellant to severe impact. This study looked at an 88% total solids HTPB/Al/AP propellant similar to what could be used in space launch boosters. The program tested propellant charges as large as 22 inches in diameter. It includes hydrodynamic modeling for developing a basic understanding of the mechanisms and to develop reliable methods for predicting explosive response of modern high solids loaded propellants. Test results will be presented showing the low velocity, low pressure reactive wave propagation and the energetic far field effects typical of these propellants when subjected to severe impact. Test results and modeling analysis will be presented illustrating interactions, not previously recognized, between burning rates and mechanical processes which produce a unique explosive response that is likely characteristic of low hazard booster propellants.

BACKGROUND

This program is jointly supported by the Titan IV System Program Office (SPO, Los Angeles AFB), the Eastern Range Safety Office (Patrick AFB) that oversees space flight operations at the Eastern Range, and the Research Triangle Institute (Cocoa Beach, FL). Personnel participating in this cooperative effort come from the Phillips Laboratory Propulsion Directorate, Edwards AFB, CA and the Lawrence Livermore National Laboratory, Livermore, CA.

The concerns of the Eastern Range Safety Office focus on the physical safety of up to 20,000 personnel on site during a space launch, the launch facilities, and people located in nearby communities. Unfortunately, failed space payload launches have finite probability that a launch vehicle could fall back to earth at unfavorable positions over an extended range. Past accidents particularly the 1986 Titan failure at Vandenburg AFB in which large atmospheric overpressure shocks were produced by solid propellant rocket motor ground impact, clearly identify the need to quantitatively assess probable explosive output of space launch systems in failed launches. Such an assessment would focus upon the 6.89 kPa (1 psi) ranges and material fragmenting traits as a function of impact velocity. A less frequent but important issue would occur if response to a solid propellant fueled booster physically disrupted a satellite's radioisotope thermoelectric generator (RTG). Satellites destined for outer planets might use RTGs for onboard electric power requirements. RTGs are powered by plutonium 238 whose dispersal would have serious environmental consequences.

Report Documentation Page

Form Approved
OMB No. 0704-0188

1. REPORT DATE	2. REPORT TYPE	3. DATES COVERED
AUG 1994		**00-00-1994 to 00-00-1994**

4. TITLE AND SUBTITLE	5a. CONTRACT NUMBER
Explosive Testing of Class 1.3 Rocket Booster Propellant	5b. GRANT NUMBER
	5c. PROGRAM ELEMENT NUMBER
6. AUTHOR(S)	5d. PROJECT NUMBER
	5e. TASK NUMBER
	5f. WORK UNIT NUMBER
7. PERFORMING ORGANIZATION NAME(S) AND ADDRESS(ES) **Phillips Lab/RKCP,4 Draco Drive,Edwards AFB,CA,93524-7160**	8. PERFORMING ORGANIZATION REPORT NUMBER
9. SPONSORING/MONITORING AGENCY NAME(S) AND ADDRESS(ES)	10. SPONSOR/MONITOR'S ACRONYM(S)
	11. SPONSOR/MONITOR'S REPORT NUMBER(S)

12. DISTRIBUTION/AVAILABILITY STATEMENT
Approved for public release; distribution unlimited

13. SUPPLEMENTARY NOTES
See also ADM000767. Proceedings of the Twenty-Sixth DoD Explosives Safety Seminar Held in Miami, FL on 16-18 August 1994.

14. ABSTRACT
see report

15. SUBJECT TERMS

16. SECURITY CLASSIFICATION OF:			17. LIMITATION OF ABSTRACT	18. NUMBER OF PAGES	19a. NAME OF RESPONSIBLE PERSON
a. REPORT	b. ABSTRACT	c. THIS PAGE			
unclassified	**unclassified**	**unclassified**	**Same as Report (SAR)**	**38**	

Since solid propellants used in large space boosters have an explosive nature, studying explosive characteristics of the ever more popular HTPB type of propellant seems an appropriate approach. This does not cover propellant filled motor cases or other gear, rather it focuses on the propellant hazards alone. Emerging space boosters and upper stages use HTPB propellants. In the future all solid propellant space boosters may use HTPB propellants. Little is known about critical diameters and explosive potentials for HTPB propellants containing 86 to 90% of combined aluminum and ammonium perchlorate solids.

HTPB/Al/AP propellants have been used in many tactical rocket weapons. Due to the small size of most tactical rocket systems as compared to space boosters little concern has been expressed for their explosive characteristics. With propellant critical diameters larger than the typical tactical missile there may not be any serious explosive concerns for smaller rocket motors.

With normal chemical explosives one might expect that transfer of full energetic yield to atmospheric shock during a chemical explosion would require that critical diameter be exceeded. As will be provided later in this paper, fully energetic atmospheric overpressure shocks can be produced by subcritical events.

Over about the last fifteen years various incidents and experimental studies have indicated that large booster propellants may be more explosive than we had thought. One example was the French report in 1988 (1) indicating that 88% solids hydroxy terminated polybutadiene - aluminum - ammonium perchlorate (88% HTPB/Al/AP) propellant had critical diameters in the range of 200 to 250 mm (8 to 10 in.) and that critical diameter for a similar 90% solids (10 HTPB/20 A1/70 AP) propellant could be as small as 83 mm (3.27 in.). In a 1992 report Merrill (2) reported that a 10,270 kg (22,600 lb.), 90% solids, HTPB/21 A1/69 AP, Super HIPPO grain donored by a conical 305 mm (12 in.) diameter, 610 mm (24 in.) long, 24.5 kg (54 lb.), C4 high explosive donor had partially reacted in violent fashion producing a very substantial crater. This result indicated that the 90% solids HTPB propellant had a critical diameter less than 305 mm (12 in.). Partial energetic yield in the Super HIPPO experiment was attributed to lack of violent initiation laterally from a directed shock. That is, supersonic shock events in a large critical diameter material have highly inhibited corner turning ability. The 1986 launch failure of a Titan III missile at Vandenberg AFB highlighted the need to improve our understanding of booster propellant explosive behavior. In that incident several large pieces of zero stage motors fell back to earth from about a 245 m (800 ft.) altitude. A number of large craters were produced in the sandy soil and atmospheric overpressure building damage indicated substantial blast effects. Metal fragments were retrieved from as far as 0.9 km (3000 ft.) from the blast site. Titan III propellant contains 84% total solids and may be our explosively safest booster propellant. The big cross sectional area of impacted solid propellant seemed to have a large influence on the degree and quantity of violence obtained.

Technology now enables us to study solid propellant explosive behavior economically. Polyvinyl difluoride piezoelectric gauges and advanced recording instrumentation now more accurately measure and record times of arrival coupled with shock magnitude measurements

and shock magnitude time histories. The LLNL has developed a reactive response computer code, called the CALE code, with systematics to predict explosive behavior in areas where actual experimentation has not been conducted. We have confidence that modification of the LLNL code will provide a better understanding using fewer experiments than a strictly experimental approach.

During the 1960s impact experiments were carried out by rocket sled impact. Hardware, range mainten-ance, and refurbishment costs involved high capital outlays and use of substantial manpower. Experimental methods for substantially sized propellant impacts have evolved from ramming a rocket motor or propellant sample on a rocket sled into a barrier, to putting impact barrier material on a rocket sled so that a static, highly instrumented test sample could more easily provide detailed data than in the moving sample impact process, to explosively driven steel plate impactors into instrumented propellant samples resting on relatively inexpensive, replaceable wooden stands. Advanced techniques in combination with computer code simulation could make very large propellant sample testing unnecessary.

The objectives for this study are to better understand the impact reactive characteristics of slow burning rate HTPB/Al/AP solid propellant, modify the LLNL CALE computer code to mimic these characteristics, and deliver the modified code to the Patrick AFB safety group so that it can be applied in improving their safety plans for solid propellant booster space flight operations at Eastern Range launch locations including the Kennedy Space Center. Vandenberg AFB should be able to take advantage of the Eastern Range safety plan if they desire. This plan should include threshold impact velocities for violent response, be adaptable to various impact surfaces, and take into account the relative sizes of propellant grains that could be involved.

DISCUSSION

The primary propellant selected for experimentation during this program is indicated by the formulation given below:

Ingredients	**Wt %**	**Notes**
HTPB polymer, additives	10.00	
DOS plasticizer	2.00	Dioctyl sebacate
Aluminum, 30 micron	19.00	Atomized
AP, 200 micron & ground	69.00	Kerr McGee, with TCP, rotary rounded

Batches of this propellant had a burn rate of 8.0 mm/second (0.32 ips) at 6.89 MPa (1000 psi) and a maximum tensile strength in the range of 500 to 750 kilopascals (kPa) (73 to 109 psi). A second booster propellant containing iron oxide that has been given only one test has the

formulation given below:

Ingredients	Wt%	Notes
HTPB polymer, additive	9.80	
DOA plasticizer	2.00	Dioctyl adipate
Aluminum, 19 micron	19.00	Atomized
Ammonium Perchlorate, 250 micron & ground	69.00	WECCO, no TCP
Iron Oxide, red, Fe_2O_3	0.20	

Burn rate of the second propellant was near 10.7 mm/sec. (0.42 ips) at 6.89 MPa (1000 psi), and its maximum tensile strength was near 689 kPa (100 psi).

Selection of booster propellant sample sizes during planning stages of the project was heavily influenced by critical diameters reported by the French in 1988 (1). Since they had reported that 88% solids HTPB/Al/AP propellant critical diameters were in the range of 200 to 250 mm, the diameters of sample cylinders were chosen to be 406 mm (16 in.) and 508 mm (20 in.) for plate impact testing. The intent was to have impact samples in excess of critical diameter or at least close to critical diameter so that substantial energetic response to impacts could be observed. With support of the LLNL computer code it was projected that even data from samples smaller than critical diameter could provide useful inputs for computer code modification. For explosive donor experiments or critical diameter tests cylindrical diameters of 203 mm (8 in.), 254 mm (10 in.), 305 mm (12 in.), 406 mm (16 in.), and 559 mm (22 in.) were selected. The majority of the explosive donor samples were of the two larger diameters since they would be more reactive due to their larger sizes. Different sizes were intended to add data about propellant energetic response dependence based on sample size.

More than 9100 kg (20,000 lbs.) of booster type propellant was cast into cylindrical samples at the Jet Propulsion Laboratory Station located on Edwards AFB. Their 570 liter (150 gallon) mixer allowed about 910 kg (2000 lbs.) of propellant to be processed per batch. Casting molds for the booster propellant cylindrical samples were cardboard paper tubes called "sono tubes" terminated at the bottom by heavy aluminum foil and tape. During casting the sono tube receptacles rested on fabricated wood stands so that they could be forklifted from the casting area to the cure ovens. Sono tubes are relatively inexpensive cardboard paper tubes commercially available in a large number of standard internal diameters ranging from 152 mm (6 in.) to 1524 mm (60 in.). Sono tubes can also be made up according to

nonstandard diameters by special order with some delay in delivery and additional cost. These sono tubes are used by the construction industry for casting concrete cylinders for ultimate load bearing strength testing. Since sono tubes are intended for making up concrete samples, they readily endure the hydraulic load of uncured propellant, even at depths of 2 meters. Prior to casting the sono tube propellant molds were lined with 0.025 mm (0.001 in.) Velostat conductive plastic sheet and sprayed with a mold release that dried leaving fine Teflon powder film on the sprayed surfaces. In this manner the cardboard tubes could be removed after propellant cure yielding free standing cylindrical samples. For those pieces of propellant that exceeded about 100 kg (220 lbs.) a band of unlined cardboard without mold release about 10 to 16 cm (4 to 6 in.) in width was exposed to the propellant as it was cast at the top of the specimen. This cardboard band bonded strongly to the solid propellant, and was used as a means of grasping the heavy propellant pieces with a special fixture for each diameter by forklift or hoist for sample movement and placement for test. Samples made of various lengths were stacked for test so that polyvinylidene difluoride (PVF2) piezoelectric and foil gauge time of arrival sensors could be placed at suitable positions between propellant pieces during test.

Our explosive experiments instrumentation devices utilized the following instrumentation devices:

PVF2 piezoelectric gauges - to measure shock time of arrival and pressure time-history

Detonation velocity probes - these were the crushing concentric resistor type placed on the exterior of samples

Foil gauges - used for time of shock arrival measurement

Crystal pins - employed in arrays along sample length measuring shock arrival times

Four Le Croy four channel high speed recorders, connected to PVF2 gauges, foil gauges, detonation velocity probes, and crystal pin arrays

PC 486 data acquisition and control system

Atmospheric overpressure sensors located at ground level at 46, 76, and 107 m (150, 250, and 350 ft.)

along about northeast and southeast legs

A 24 track tape recording system for overpressure sensor recording

Three - 30 frame per second video cameras

One - 1000 frame per second color film camera

A 20,000 picture per second Photec color film camera (half framed at 10,000 frames per second)

A 40,000 picture per second NAK color film camera (quarter framed at 10,000 frames per second)

One or two C4 explosive driven argon flash units of 4.9 m length (16 ft) with a 387 mm (15.25 in.) square cross section, about one millisecond duration per flash unit

Mirror to provide sample illumination for camera observed areas in shadow by light from the flash units, variable widths and variable heights of 1.22 or 2.44 m (4 or 8 ft)

Grid with 15.24 cm (6 inch) divisions for size calibration on photographs, usually made of 2.44

by 2.44 m (8 by 8 ft) or 1.22 by 2.44 m (4 by 8 ft) particle board

Explosive initiation systems using exploding bridgewires initiators (EBWs) were used initially. Since our explosive test ground zero is located about 1800 feet from our blockhouse, a low voltage system for transferring control of the EBW system within 107 m (350 ft.) of ground zero introduced electrical vulnerability that is not a characteristic of the standard EBW system. As a consequence, our explosive initiation systems have evolved. A second system moved the EBW initiation completely into the blockhouse and test initiation was carried from an EBW just outside the blockhouse by detonation cord to the test articles and argon flash units. Our latest system uses "noiseless trunkline" by Ensign Bickford that allows manual initiation from within the blockhouse and initiation signal transfer through a small plastic tube about 2 mm (0.08 in.) in diameter to the test article and argon flash units. Noiseless trunkline acts similar to detonation cord at a 1980 m/sec. (6500 ft./sec.) rate, but can be held in the hand without injury. The electrical immunity of noiseless trunkline and the complete absence of any electrical firing initiation controls in the noiseless trunkline system provides much greater safety. Another very significant advantage is that mechanical noiseless trunkline operation also eliminated about two thirds of checklist items in our tedious countdown procedure. A breakwire in the trunkline close to the blockhouse starts high speed cameras; a 1.5 second delay detonator in the noiseless trunkline allows the high speed cameras to get up to speed; and the delay detonator starts the initiation blast signal through lines branched to the test article and the flash units while triggering readiness of the Le Croy high speed recorders. Synchronization of activities close to ground zero is controlled by careful selection of lengths of noiseless trunkline.

Figure 1 shows a diagram of our typical explosive or impact test site. Test articles are placed at ground zero located about 550 meters (1800 ft.) E by SE from the control bunker. Two legs of three atmospheric overpressure gauges in about the NE and SE directions are positioned at 46, 76, and 107 m (150, 250, and 350 ft.) from ground zero. Three high speed film cameras are set about SW of ground zero at a distance of 64 meters (210 ft). Two 30 frame per second video cameras are located out of line and behind the high speed cameras at

a range of about 150 m (500 ft). An electric terminal box below ground level housing the Le Croy recorders was about N by NW from ground zero at a distance of 107 m (350 ft). One or two C4 explosively driven argon flash units were placed in the westerly direction from ground zero at distances between 18 to 34 m (60 to 110 ft.). Approximately 15 m (50 ft.) from the flash units argon cylinders are placed in buried steel boxes and provide argon gas flow through plastic tubing to feed the flash units. Argon flow at about 70 liters per minute is supplied to the flash units for at least 1 hour prior to explosive trials to fill the units with argon. Directly opposite the cameras and about 3 m (10 ft.) behind the test article is set, typically, a 2.4 by 2.4 m (8 by 8 ft.) particle board painted with grid markings spaced 152 mm (6 in.) apart. At a range of about 3 m (10 ft.) to the east of the test article is placed a 2.4 by 2.4 m (8 by 8 ft.) mirror angled so that light from the flash units can be reflected onto the part of the test article that would be observed by the cameras but be in the shadow of direct light from the flash units.

First explosive testing of our primary booster propellant was a critical diameter test of a 203 mm (8 in.) outer diameter cylinder by 813 mm (32 in.) in length. Propellant weight was 47.7 kg (105 lbs.). C4 high explosive was used as donor with a diameter of 197 mm (7.75 in..) and a depth of 102 mm (4 in.). C4 weight was 4.99 kg (11 lbs.). Initiation of the C4 was accomplished by seven equally spaced nonelectric caps stimulated by detonation cord strands of equal length coming out of a 0.91 kg (2 lb.) ball of C4 explosive. The sample propellant cylinder was resting vertically on a 102 mm (4 in.) block of paraffin that was in turn set on a 19 mm (0.75 in.) piece of plywood about 0.91 m (3 ft) square. A pair of EBWs set at the top of a wood board driven into the soil initiated a 1.27 m length of detonation cord that terminated in the C4 ball attached to the seven detonation cords of the multipoint explosive initiation system. See Figure 2 for an explanation of the test components at ground zero.

Instrumentation for the 203 mm diameter experiment consisted of two detonation velocity probes, four PVF2 gauges placed at an edge and center of the propellant at top and bottom of the sample cylinder, atmospheric shock overpressure gauges, six crystal pins equally spaced down the side of the propellant cylinder, a Photec 40,000 pictures per second camera, an argon flash unit of 305 mm square cross section by 2.44 m long, and a single color video camera. See Figure 3 to see where detonation probe, PVF2 sensors, and crystal pins were placed on the 203 mm diameter test sample.

Figure 1. Site Plan for Explosive Tests (not to scale)

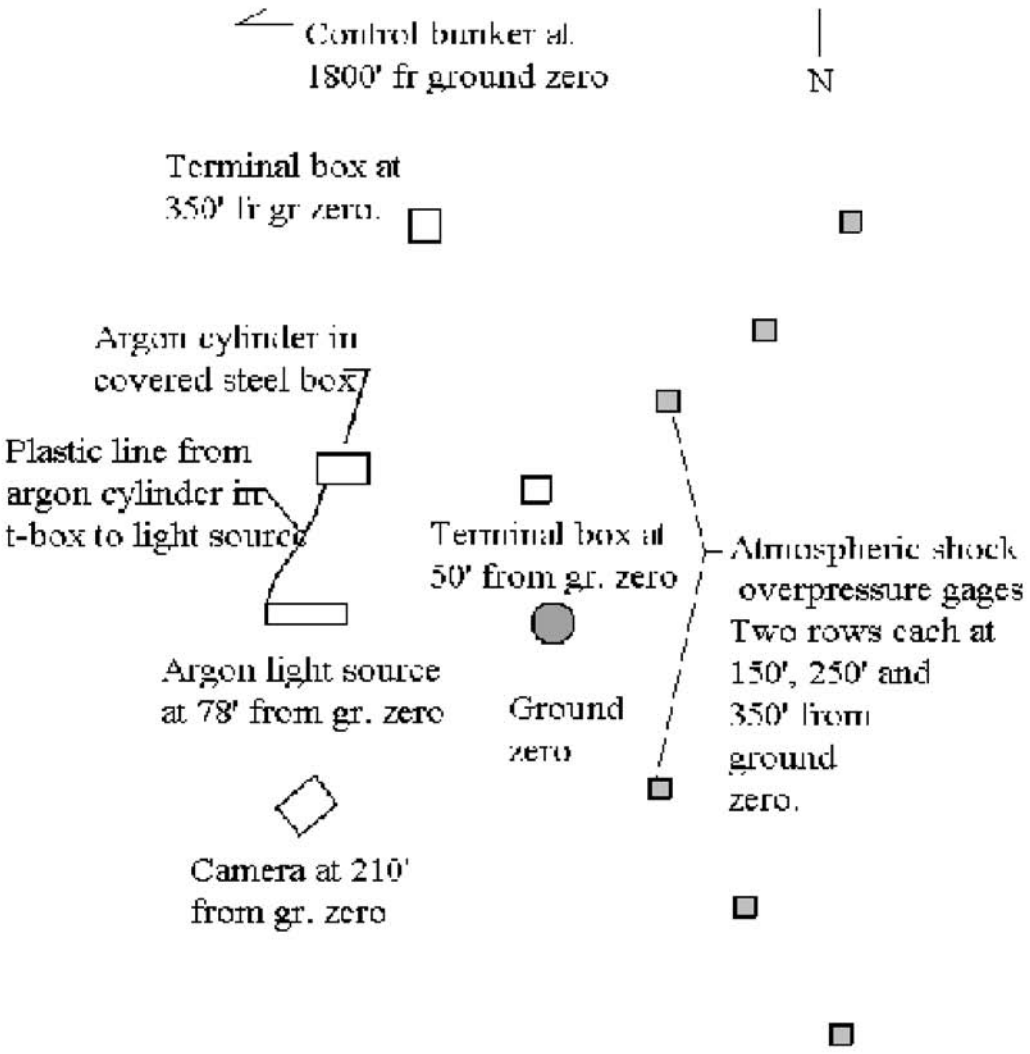

Figure 2. 8 in. Critical Diameter Test Configuration

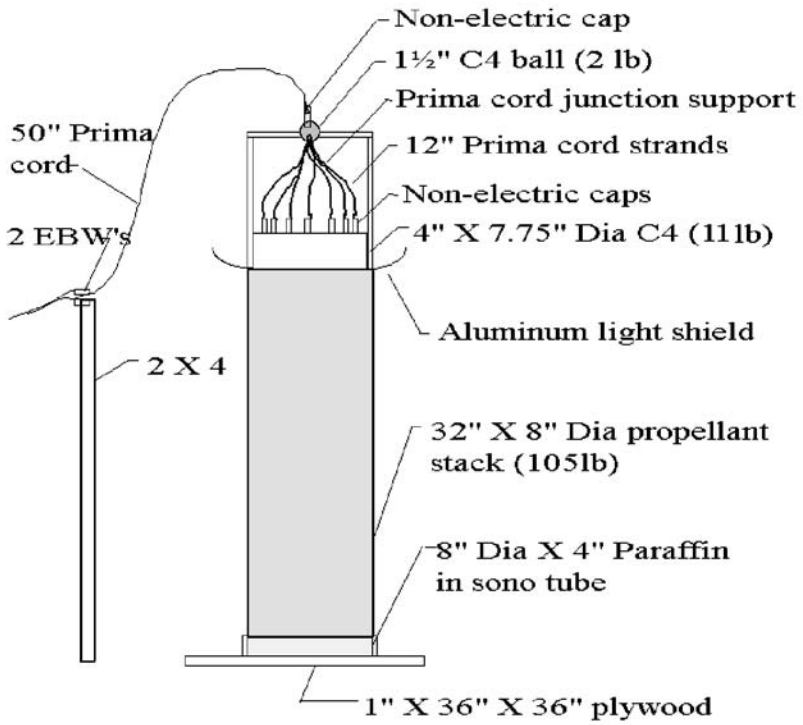

Figure 2.
Eight-inch Critical Diameter Test Configuration

Figure 3. 8 in. Test Sensor Positions

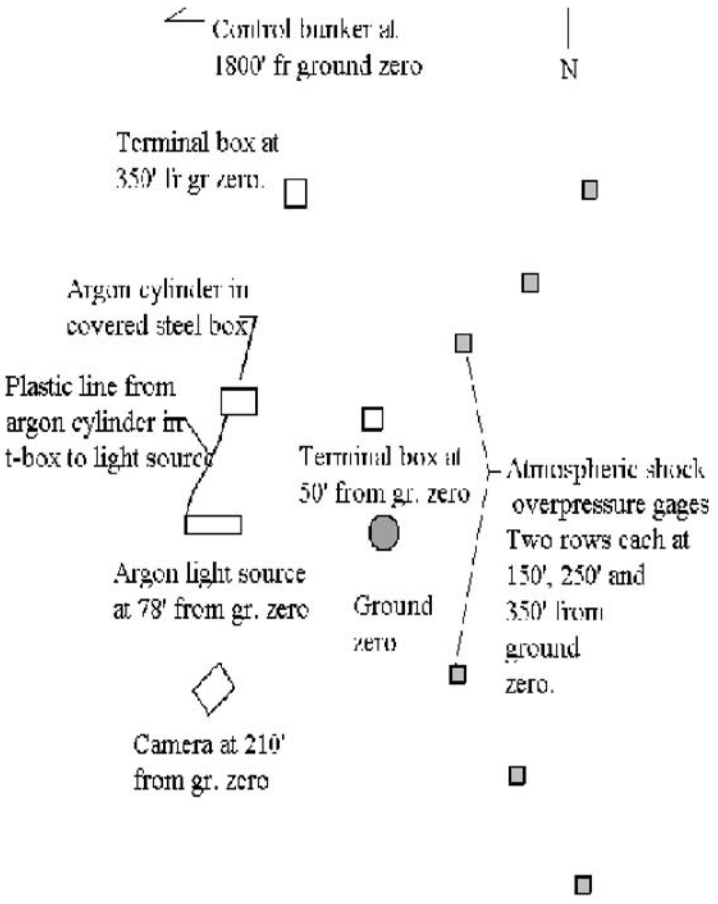

No crater was produced by the 203 mm diameter propellant sample with the C4 donor. Rather surprisingly, the atmospheric overpressure yield was about that expected for the combination of about 5 kg (11 lbs.) of C4 and 48 kg (105 lbs.) of aluminized solid booster propellant should it have completely detonated. E.g., 5 kg (11 lbs.) C4 times 1.19 TNT factor plus 48 kg (105 lbs.) propellant times 1.3 TNT factor or about 68 kg (149 lbs.) of TNT eguivalency. See Table 1 for a listing of overpressure data that was obtained. High overpressure yield was obtained despite observation of some burning propellant pieces being thrown clear from ground zero. Since no detonation of propellant had occurred, the test demonstrated that slow burning, aluminized, HTPB propellant could give high atmospheric overpressure shocks without being involved in detonation behavior.

TABLE 1. Eight Inch Critical Diameter Atmospheric Shock Data

Direction	Radius meters (ft)	Arrival Time (millisecs)	Overpressure Peak, kPa, (psig)
NE	46 (150)	100.8	13.0 (1.89)
SE	46 (150)	100.2	11.6 (1.69)
NE	76 (250)	183.6	8.20 (1.19)
SE	76 (250)	184.0	6.50 (0.943)
NE	107 (350)	268.4	4.24 (0.615)
SE	107 (350)	268.8	4.03 (0.585)

TABLE 1. Eight Inch Critical Diameter Atmospheric Shock Data

At a later time an overpressure gauge calibration experiment was conducted with a 203 mm (8 in.) diameter by 711 mm (28 in.) long cylinder of carefully packed C4 high explosive in a cardboard sono tube. Weight of the C4 explosive cylinder was 37.3 kg (82 lbs.). Length to diameter ratio was 3.5. This length to diameter ratio was the same as for the 559 mm (22 in.) critical diameter test including the high explosive donor and somewhat shorter than the 4.5 overall length to diameter ratio employed in the 8-in. critical diameter trial. The C4 charge stood vertically on top of a wood rack about 178 mm (7 in.) high and a 76 mm (3 in.) thick disc of paraffin.

An array of seven equally spaced nonelectric caps connected to a central ball of C4 explosive by equal lengths of detonation cord was used for calibration trial explosive initiation. Primary explosive initiation was by a pair of EBWs against a single 1.07 m (3.5 ft.) length of detonation cord leading to the C4 ball and multipoint initiation system. Figure 4 is a diagram of the C4 charge configuration for the overpressure gauge calibration experiment. Table 2 below contains overpressure measurements made during the calibration event.

Figure 4. Overpressure Calibration Trial Configuration

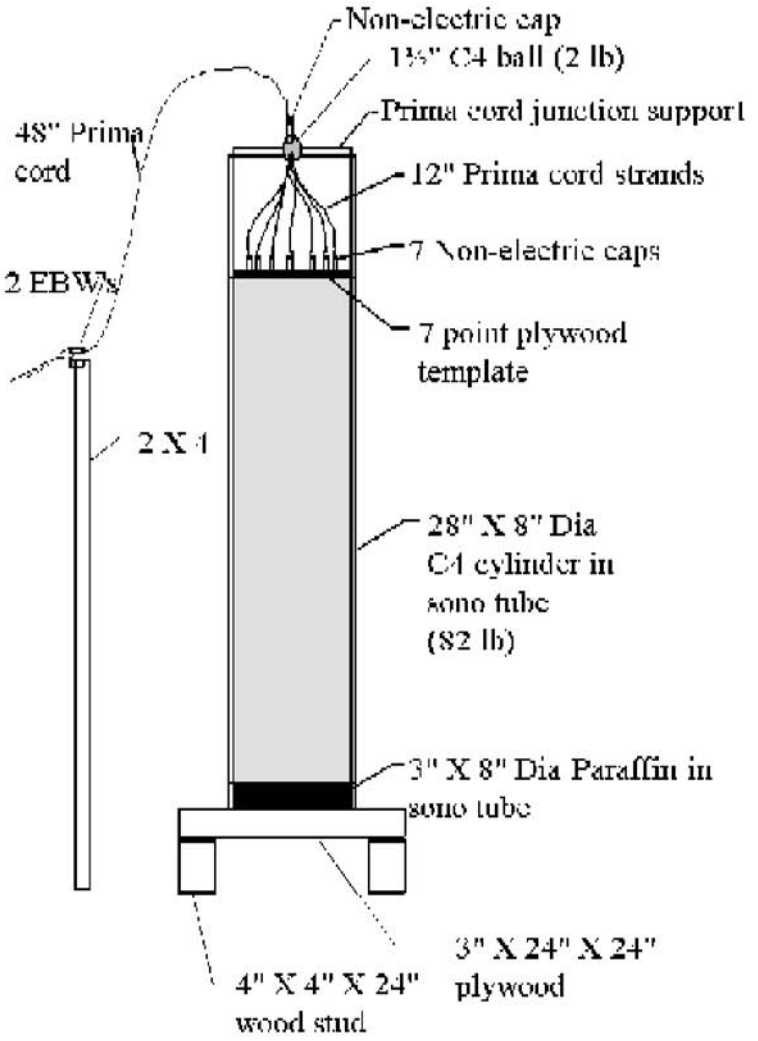

Figure 4.
C4 Overpressure Calibration Trial Configuration

Table 2. 8-in. C4 Overpressure Calibration Trial

Direction	Radius, m (ft)	Arrival Time, millisecs	Overpressure Peak, MPa (psig)
NE	46 (150)	102.7	10.7 (2.56)
SE	46 (150)	102.0	9.58 (1.36)
NE	76 (250)	184.4	5.37 (0.779)
SE	76 (250)	186.7	4.64 (0.673)
NE	107 (350)	272.3	3.47 (0.504)
SE	107 (350)	268.7	3.07 (0.446)

Table 2. 8-in. C4 Overpressure Calibration Trial

Overpressures are in fair aqreement with the expected TNT equivalency of 37.3 kg (82 lbs.) times 1.19 TNT factor or 44.4 kg (97.6 lbs.) of TNT equivalency.

From the 8-in. critical diameter test only the PVF2 gauge at the bottom of the propellant sample provided data. This was a time of arrival of 271.8 microseconds after EBW initiation and a shock of 3.9 kilobars. If the time for the initiation system to traverse 157.5 mm (62 in.) of detonation cord and 101.6 mm (4 in.) of C4 donor explosive is subtracted out, an average shock velocity through the 813 m (32 in.) of propellant was a little less than 3 mm per microsecond. This crude number agreed approximately with the limited crystal pin data received as given below in Table 3:

Table 3. 8-in. Critical Diameter Test Crystal Pin Times of Arrival

Pin No.	Time of Arrival, microseconds	Distance	Velocity Thru Interval, mm/microsec
CPl	-0-	0	-
CP2	49.8	162.6	3.3
CP3	113.1	325.6	2.6
CP4 etc.	-	-	-

Table 3. 8-in. Critical Diameter Test Crystal Pin Times of Arrival

Thus, shock velocity through the propellant was slow compared to any expected detonation velocity and seemed to be fading.

In Figure 5 is shown the experimental arrangement for the 559 mm (22 in.) critical diameter test. Total length of our primary propellant sample was 1760 mm (69.3 in.). At the bottom of the propellant sample stack were five short propellant cylinders having a height of 172 mm (6.78 in.) each. Above the short cylinder stack was a single propellant piece of 857 mm (33.8 in.) length. This heavy piece had a 152 mm (6 in.) wide band of sono tube bonded to its

upper perimeter that was used as a means of grasping the propellant piece for lifting in transportation and placement for test. Total propellant weight was 778 kg (1712 lbs.). Thin Velostat sheet (0.03 in.) was wrapped around the sample and grounded for improved electrostatic safety. Similar to previous cylinder tests, the propellant sample rested upon a 178 mm (7 in.) high wood rack and a 76 mm (3 in.) thick sheet of paraffin. To keep the heavy sample assembly from sinking into the soil at ground zero a sheet of plywood 19 mm (0.75 in.) thick and 1.22 m (4 ft.) square was placed upon the ground under the sample assembly. On top of the vertical standing sample was placed a 127 mm (5 in.) thick disc of C4 donor explosive 546 mm (21.5 in.) in diameter. C4 weight was 47.7 kg (105 lbs.). A 19 mm (0.75 in.) thick sheet of particle board 533 mm (21 in.) in diameter served as a template for a 19 point initiation system with nineteen holes drilled through it. During test preparation the template sheet was laid upon the C4 donor charge and 19 nonelectric caps attached to equal lengths of detonation cord were inserted into the holes. The nineteen 508 mm (20 in.) length detonation cords were taped together and inserted into a 38 mm (1.5 in.) diameter ball of C4 explosive taped to a lightweight wood support. A single strand of 1.07 m (3.5 ft.) long detonation cord led to the C4 ball from a pair of EBW initiators.

Figure 5. 22-in. Critical Diameter Test Configuration

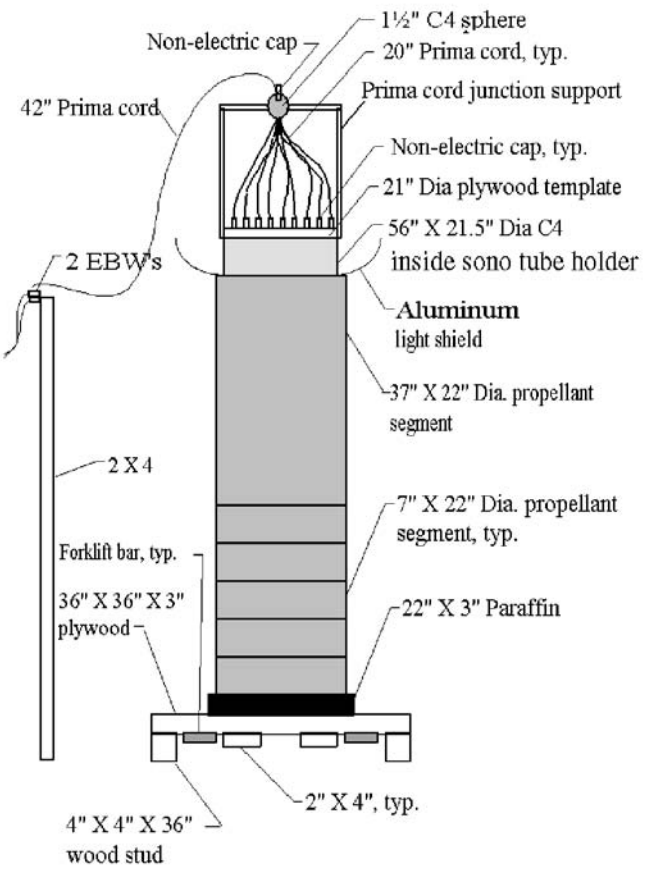

Figure 5.
Twenty-two Inch Critical Diameter Test Configuration

Positions of sensors for the 22-in. critical diameter test sample are indicated in Figure 6. Two vertical rows of eleven crystal pins 180 degrees apart were employed. Crystal pin rows started 236 mm (9.3 in.) from the top of the propellant cylinder and were spaced 152 mm (6 in.) apart. Twelve PVF2 gauges were installed with three at each of four levels. The PVF2 gauges were at top, 940 mm (37 in.) down, 1473 mm (58 in.) down, and bottom of the propellant cylinder. At each PVF2 level gauges were set along a line at center, half radius, and edge of the propellant sample. Upward from the sample bottom and 180 degrees apart were placed two crushing resistor, detonation velocity probes. One probe was 610 mm (24 in.) long and the other was 1220 mm (48 in.) long.

Figure 6. 22 in. Test Sensor Positions

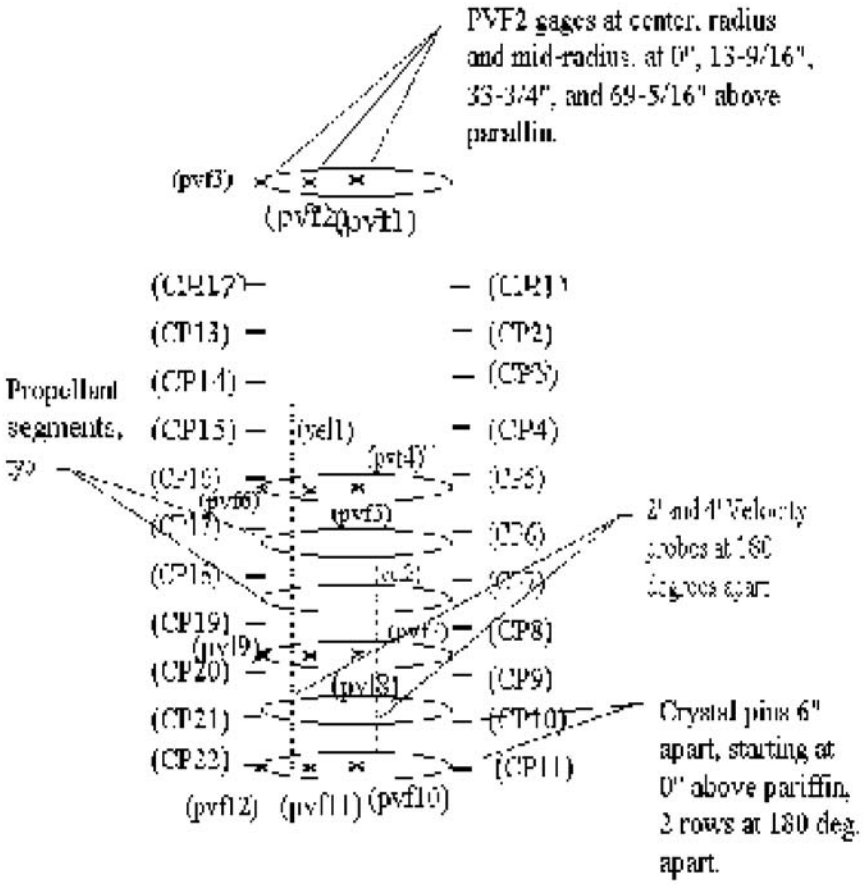

Figure 6.
Twenty-two Inch Test Sensor Positions

When the 22-in. critical diameter test was conducted, high atmospheric overpressures were observed, some flaming propellant fragments were observed, and the 19 mm (0.75 in.) thick plywood board upon which the propellant and supports rested was not punctured. Unfortunately, only three overpressure measurements were obtained since a burning propellant fragment severed wires within a terminal box about 50 ft. from ground zero. Acceptable 34,000 quarter frames per second photographs were obtained showing shock/flame front progression down the length of the propellant sample. Crystal pin data, for the most part, was very consistent, detonation velocity probe data was fairly indecipherable, and PVF2 gauge data was analyzed with some difficulty. Although lack of detonation was indicated by absence of a crater and surviving piece of plywood support, relatively high energy yield was transferred into atmospheric shock. See Table 4 below for atmospheric

overpressures:

Table 4. 22-in. Critical Diameter Test Overpressures

Direction	Distance Meters (ft.)	Arrival Time, Mi11iseconds	Peak Overpressure, kPa (psig)
NE	46 (150)	----	----
SE	46 (150)	72.65	7.22
NE	76 (250)	149.61	3.44
SE	76 (250)	149.41	3.01
NE	107 (350)	----	----
SE	107 (350)	----	----

Table 4. 22-in. Critical Diameter Test Overpressures

Overpressures above suggest a TNT equivalency of about 950 kg (2100 lbs.). Estimation of TNT yields based on overpressures would be about 778 kg of propellant times 1.3 plus 48 kg of C4 times 1.19 for an estimated total of 1070 kg (2350 lbs.) TNT equivalent. Overpressures obtained were roughly 90% of estimated maximum energetic yield.

Shock velocities derived from crystal pin time of arrivals are given below in Table 5. Pins were numbered from 1 to 11 in one vertical line and from 12 to 22 in a second line 180 degrees away on the sample. As can be seen a fading shock ranging from about 4 mm per microsecond down to just above 2 mm per microsecond near the bottom end of the propellant cylinder was observed.

Table 5. 22 -in. Test Shock Velocities From Crystal Pins

Ending at Pin No.	Velocity, mm/microsec	Ending at Pin No.	Velocity, mm/microsec
2	4.2	13	4.2
3	3.9	14	1.9?
4	3.6	15	3.4
5	3.2	16	2.7
6	3.0	17	2.8
7	2.5	18	2.5
8	2.3	19	2.8
9	2.5	20	2.3
10	2.1	21	2.6
11	2.3	22	2.5

Table 5. 22 -in. Test Shock Velocities From Crystal Pins

Table 6 below displays values for PVF2 gauges placed in the 22-in. critical diameter test.

Table 6. 22-in. Diameter Test PVF2 Data

Gauge	Distance mm	Distance Delta mm	Time of Arrival From EBWs microsec	Delta	Inline Shock Velocity mm/microsec	Peak Pressure kbar
Center						
PVF1	0	0	-	-	-	-
PVF4	903.3	903.3	1010.	-	-	-
PVF7	1416.1	512.8	1237.6	127.6	4.02	13.7
PVF10	1760.5	344.4	1412.1	174.5	1.97	4.3
Mid Radius						
PVF2	0	0	-	-	-	-
PVF5	903.3	903.3	1026.5	-	-	38.6?
PVF8	1416.1	512.8	12588.8	232.3	2.21	2.4
PVF11	1760.5	344.4	-	-	-	-
Outer Radius						
PVF3	0	0	-	-	-	-
PVF6	903.3	903.3	1043.	-	-	10.7
PVF9	1416.1	512.8	1243.5	200.5	2.56	9.8
PVF12	1760.5	344.4	1412.6	169.1	2.04	3.3

Table 6. 22-in. Diameter Test PVF2 Data

PVF2 gauges gave pressures that are somewhat suspect in value until we can determine how much signal contribution came from strain of the gauges during the explosive event. An interesting factor was the appearance of a second, more sustained, and stronger pulse following the first pressure pulse by about 30 to 65 microseconds. See Figure 7 for a record showing a second pressure following the first by about 65 microseconds. Computer modeling of the propellant reactive processes can show similar behavior as discussed later. At this time it is uncertain whether this second pulse is enhanced by an electrical signal produced by mechanical strain of the PVF2 gauge. Future testing awaits resolution by utilizing strain gauge and PVF2 pairs in a similar environment.

A series of quarter frame photos at 34,000 pictures per second exhibited a relatively steady progression of reaction flame front down the length of the 22 in. sample. Measurements taken off the photos gave varying results frame to frame due to difficulty resolving a relatively fuzzy leading edge to the flame front. Since the propellant cylinder was wrapped with a layer of thin Velostat plastic sheet, its contribution to camera viewing distortion of the flame front is not known. Overall, an average velocity over the total sample was about 2.4 mm per microsecond. This velocity basically agrees with data from the crystal pin and PVF2 gauge times of arrival.

Figure 7.
PVF2 Record at Half Radius 903 mm from Top of 22-in. Propellant Cylinder

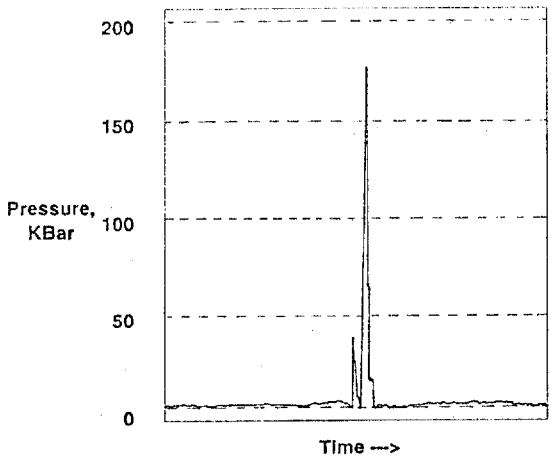

Figure 7. PVF2 Record at Half Radius 903 mm from Top of 22-in. Propellant Cylinder

A 406 mm (16 in.) critical diameter experiment was conducted with our second propellant that contains iron oxide and had a higher burn rate (10.7 mm/sec, 0.42 ips at 6.9 MPa) than for our primary propellant. Several changes were made in the test configuration. The biggest change was to utilize an ammonium perchlorate (AP) explosive donor rather than a C4 donor. In previous work looking at explosive properties of AP detonation shock velocities were about 3 to 4 mm/microsec. and estimated shock intensity was about that observed in solid propellant reactions, 35 to 45 kilobars. It seemed possible that explosive transition from the AP to the propellant would occur without the strong overdriving provided by C4 explosive. In addition, long shock times were desired since our experimentation was intended to give some insights into processes that would occur in propellant during failed launch fall back events that would have long shock periods upon collision with the earth. To obtain a longer initial shock period the AP donor was made 1067 mm (42 in.) deep at 406 mm (16 in.) diameter. Another change was the addition of 203 mm (8 in.) and 102 mm (4 in.) wide bands of soft aluminum around the AP and propellant sample cylinders, respectively. Aluminum bands were an attempt to gain photographic information on lateral accelerations of the AP and propellant due to an explosive event. Lateral acceleration is a parameter that can be used by the LLNL reactive response code. Explosive initiation of the AP was accomplished by two EBWs on the end of a 1.22 m (48 in.) length of detonation cord leading to a hemispherical C4 explosive charge buried at the surface of a 305 mm (12 in.) diameter by 152 mm (6 in.) depth of AP resting atop a thin sheet of wood centered upon the main AP charge that had a diameter the same as the propellant sample and a length of 1067 mm (42 in.). The propellant sample was made up of a top segment 305 mm (12 in.) long, a mid segment 102 mm (4 in.) long, and a bottom segment 406 mm (16 in.) long. Total sample and initiating charge structure were set upon a 76 mm thick by 0.91 m square wood sheet supported from the ground by a pair of 76 mm square by 0.91 m long wood pieces. Figure 8

shows a sketch of the 16-in. critical diameter test configuration.

Sensors attached to the 16-in. test with the iron oxide propellant have their positions indicated in Figure 9. These included three foil gauges set at the top of the main AP charge, at the end of the main AP donor charge/beginning of the propellant sample, and at the end of the propellant sample. Two vertical rows of twelve crystal pins were positioned 180 degrees apart on the upper half of the propellant sample with 25.4 mm (1 in.) spacings starting 25.4 mm down from the top of the propellant sample and skipping three positions below the sixth pin where a soft aluminum expansion band was placed. Crystal pins were embedded into the propellant to a depth of 25 mm. Nine PVF2 gauges were used. Two PVF2 gauges were set on center surrounded by AP atop a 3 mm thick sheet of Velostat conductive plastic 28 mm (1.1 in..) up from the top of the propellant sample. Another PVF2 gauge was put on the propellant top 25 mm from the outer edge. Two more sets of three PVF2 gauges, two at center and one near the propellant edge were placed at distances down from the propellant sample top at 305 mm (12 in.) and 406 mm (16 in.). The last sensor, a 610 mm (24 in.) crushing resistor detonation probe was set starting downward from the propellant sample top.

Figure 8. 16-in. Diameter Test Configuration

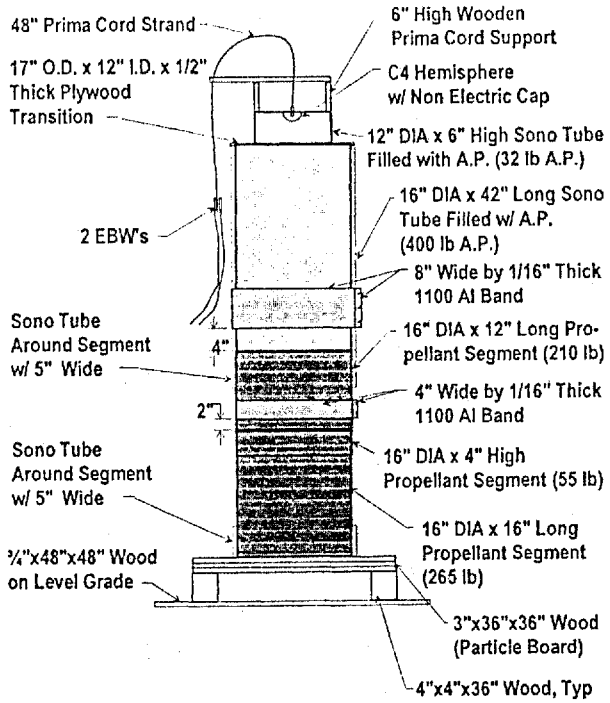

Figure 8. 16-in. Diameter Test Configuration

Figure 9. 16-in. Test Sensor Positions

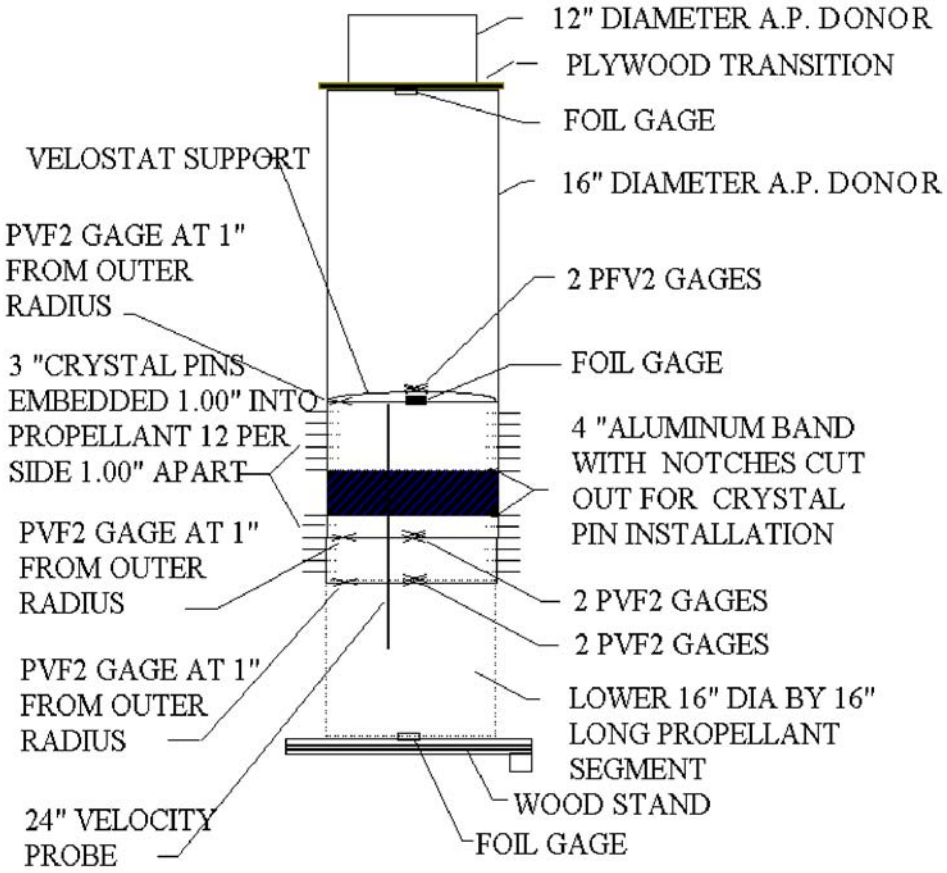

Figure 9.
Sixteen Inch Test Sensor Positions

Cameras and atmospheric overpressure sensors did not record the event when the 16-in. test was initiated. As a result, aluminum band lateral expansions and TNT yields were not obtained. No evidence of unburned propellant pieces or of new aluminum oxide spots indicating propellant fragment burning was observed. However, high speed sensors, crystal pins, PVF2 gauges, and detonation probe gave signals. Detonation probe output was quite noisy. This detonation probe noise may have occurred because shock pressures at the propellant surface were low. Pressures reported by PVF2 gauges at the edge of the propellant sample were about 1.8 kbar at the beginning increasing to about 15 kbar at 406 mm down the sample. Although all PVF2 gauges gave times of arrival, an unprotected sensor just above the sample in the AP and a sensor at the top edge of the propellant did not give readable pressure signals. See Table 7 for crystal pin and foil gauge data and Table 8 for PVF2 data. From these data a substantial difference in times of arrival amounting to several microseconds between the response of crystal pins and PVF2 gauges can be detected. Within each type of sensor calculated velocities seem to agree.

Table 7. 16-in. Diameter Crystal Pin and Foil Gauge Data for Iron Oxide - HTPB Propellant

Sensor	Diameter to 1st AP Foil mm	Delta mm	Time of Arrival microsec.	Delta	Internal Velocities mm/microsec.
Foil CAP	0	----	0	0	----
Foil CAP/P	1054.1	1054.1	341.5	341.5	3.09 AP
CP1 Prop	1079.5	25.4	453.7	13.2	1.92?
CP2 Prop	1104.9	25.4	360.1	5.4	4.70
CP3 Prop	1130.3	25.4	366.4	6.3	4.03
CP4 Prop	1155.7	25.4	374.0	7.6	3.34
CP5 Prop	1181.1	25.4	380.1	6.1	4.16
CP6 Prop	1206.5	25.4	386.6	6.5	3.91
CP7 Prop	1308.1	101.6	416.1	29.5	3.44
CP8 Prop	1333.5	25.4	423.6	7.5	3.39
CP9 Prop	1358.9	25.4	431.1	7.5	3.39
CP10 Prop	1384.3	25.4	439.5	8.4	3.02
CP11 Prop	1409.7	25.4	448.2	8.7	2.92
CP12 Prop	1435.1	25.4	456.6	8.4	3.02
Foil C Prop	1866.9	431.8	615.3	158.7	2.72
Foil CAP/P	1054.1	812.8	341.5	273.8	2.97
CP13 Prop	1079.5	25.4	354.9	13.4	1.90?
CP14 Prop	1104.9	25.4	361.2	6.3	4.03
CP15 Prop	1130.3	25.4	366.9	5.7	4.46
CP16 Prop	1155.7	25.4	372.7	5.8	4.38
CP17 Prop	1188.1	25.4	379.5	6.8	3.74
CP18 Prop	1206.5	25.4	386.4	6.9	3.22
CP19 Prop	1308.1	101.6	415.9	29.5	3.44
CP20 Prop	1333.5	25.4	423.3	7.4	3.43
CP21 Prop	1358.9	25.4	432.5	9.2	2.76
CP22 Prop	1384.3	25.4	441.0	8.5	2.99
CP23 Prop	1409.7	25.4	458.8	8.9	2.85
CP24 Prop	1435.1	25.4	458.8	8.9	2.85
Foil C Prop	1866.9	431.8	615.3	156.5	2.76

CAP = Center of ammonium perchlorate donot
CAP/P = Center at interface between AP and propellant sample
Prop = In propellant

Table 7. 16-in. Diameter Crystal Pin and Foil Gauge Data for Iron Oxide - HTPB Propellant

Table 8. 16-in. Diameter PVF2 Data for Iron Oxide

Sensor	Diameter to 1st AP Foil mm	Delta mm	P kbar	Time of Arrival microsec.	Delta	Interval Velocities mm/microsec.
Foil CAP	0	0	--	0	0	--
PVF2 CAP	1026.2	1026.2	--	336.5	226.5	3.05 AP
PVF2 CAP	1026.2	1026.2	35.2	334.7	334.7	3.07 AP
PVF2 EAP/P	1054.1	1054.1	--	354.9	354.9	2.97
PVF2 CAP	1358.9	332.7	--	426.5	91.8	3.62
PVF2 CP	1358.9	332.7	--	426.8	90.3	3.68
PVF2 EP	1358.9	304.8	8.8	437.8	82.9	3.68
PVF2 CP	1454.2	95.3	20.7	457.1	30.6	3.11
PVF2 CP	1454.2	95.3	11.4	456.9	30.1	3.17
PVF2 EP	1454.2	95.3	15.3	457.1	29.3	3.25

CAP = Center of ammonium perchlorate
CP = Center of propellant
EAP/P = Edgee of the AP and propellant interface
EP = 25.4 mm (1 in.) from edge of the propellant

Table 8. 16-in. Diameter PVF2 Data for Iron Oxide

In contrast with the 22-in. test using the primary test propellant a small crater was formed by the 16-in. diameter experiment using our second test propellant. The crater was about 0.23 m (9 in.) deep by about 0.76 m (30 in.) diameter. A relatively small shock velocity difference at the bottom of the propellant cylinders, e.g., about 2.3 mm/microsec. for the 22-in. test and 3.1 mm/microsec. for the 16-in. test, seems to correlate with considerable difference in cratering ability in an explosive event. Since crystal pins and PVF2 gauges indicated slowing of explosive shock through the 16-in. diameter propellant sample, a detonation was not observed; but a slightly larger diameter might provide a steady shock event. A rough estimate based on the 22-in. and 16-in. critical diameter test data would conclude that critical diameters of the two propellants might differ by a factor of two. Relatively small changes in the formulations and in propellant burn rates are responsible for the substantial critical diameter differences. Elucidation of factors contributing to the sizable critical diameter differences for the two propellants awaits support for a more extended experimental program.

At the beginning of the program it was recognized that an economical approach to booster propellant impact studies was desired as compared to rocket sled impacts. This would entail low cost acceleration and facility refurbishment techniques and a static, highly instrumented propellant sample for acquiring a rich array of data. The Gurney approach for producing high speed steel plates by setting off a sheet of high explosive sandwiched between steel plates seemed attractive. Upon review the second free flying steel plate seemed unnecessary, and one plate for impacting the samples driven by a substantially larger quantity of driver explosive seemed appropriate. This was favorable since one destructive heavy fragment was removed from the impact experiments. By configuring the system so that the impact plate was driven vertically downward lateral flight of the steel impact plate or an impact plate fragment would be minimized. See Figure 10 for a sketch indicating driver charge, wood buffer material for minimizing plate distortion, steel plate, propellant sample, etc.

Two above ground plate impact experiments have been carried out. The second of the plate impact trials will be described here to provide an example of how they are conducted and results that were obtained. Components supporting the driver charge, steel impact plate, and our primary propellant sample are made of wood, wood dowels, and adhesives to avoid long range, high speed fragments dangerous to our close-in (64 m, 210 ft.) high speed cameras. Legs were constructed of 102 by 102 mm (4 by 4 in.) wood beams. A 178 mm (7 in.) thick table rested atop four legs that was used as a platform for a 1.22 mm (48 in.) diameter driver charge of AP 203 mm (8 in.) deep encircled by a 305 mm (12 in.) high cardboard tube, adhesive held a 76 mm (3 in.) thick by 0.61 m (24 in.) diameter, 175 kg (385 lbs.), steel impact plate on the table bottom, and attached were three wood dowel tensile members supporting an underslung wood platform for placement of a 508 mm (20 in.) diameter by 508 mm (20 in.) long propellant sample weighing 185 kg (408 lbs.) located 102 mm (4 in.) below the steel plate. The bottom of the propellant sample was located 48 m (19 in.) above ground level. A soft aluminum, 102 mm (4 in.) wide band was placed around the propellant sample with the top edge positioned 248 mm (9.75 in.) below the top of the sample cylinder. This band was intended to provide photographic information about sample lateral acceleration during the impact event useable by the CALE computer code if the image was not obscured

by a debris cloud produced by the event. Explosive initiation was conducted through a noiseless trunkline system to 19 simultaneous, individual detonators resting against a 6.4 mm (0.25 in.) thick sheet of DuPont DETA sheet resting on the upper surface of AP driving charge of 203 mm (8 in.) thickness.

Figure 10. Plate Two Test Configuration

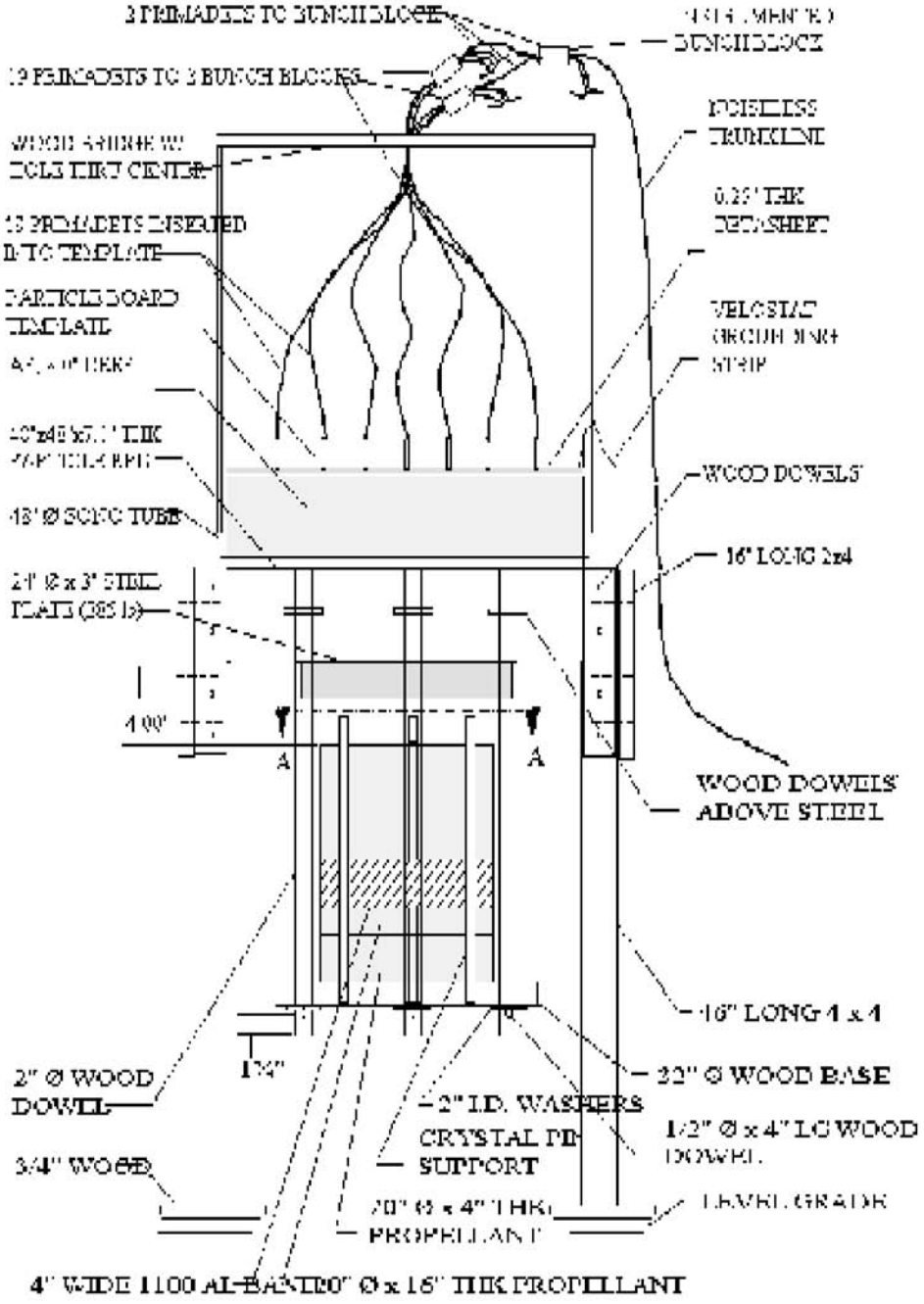

Figure 10.
Plate Two Test Configuration

Figure 11 indicates positions of sensors put on the propellant sample in the Plate 2 test. A pair of PVF2 gauges were set at each of three locations, top, 305 mm down from the top at a separation in the propellant sample, and bottom of the propellant cylinder 406 mm down from the top. Two PVF2 gauges were set at the propellant separation 25 mm (1 in.) from the outside surface of the propellant. One additional PVF2 gauge was set under the propellant sample bottom 25 mm (1 in.) from the sample cylinder outer surface. One vertical row of 10 crystal pins was placed on the sample cylinder starting at 38 mm (1.5 in.) from the top with a spacing of 38 mm (1.5 in.). The vertical crystal pin array was interrupted between 229 mm (9 in.) and 356 mm (14 in.) to allow placements of a 102 mm wide soft aluminum band around the sample cylinder that was hoped to be seen expanding during the plate impact event. Four crystal pins were set just outside the radius of the propellant sample with the first crystal pin 10 mm below the impact plate and with successive 10 mm vertical spacings between the crystal pins. The four plate velocity meauring crystal pins were placed about equidistant between two pairs of three sets of crystal pins with 120 degree spacings intended to detect plate tilt at impact. Spacings for the three sets of tilt measuring crystal pins were at 2.7 and 14.2 mm (0.15 and 0.557 in.), 5.3 and 16.3 mm (0.208 and 0.653 in.) and 4.2 and 16.7 mm (0.165 and 0.659 in.) vertically above the propellant sample cylider top, respectively. A pair of crushing resistor type detonation velocity probes of 508 mm (20 in.) length were placed vertically on opposite sides of the propellant sampls.

Figure 11. Plate 2 Test Sensor Positons

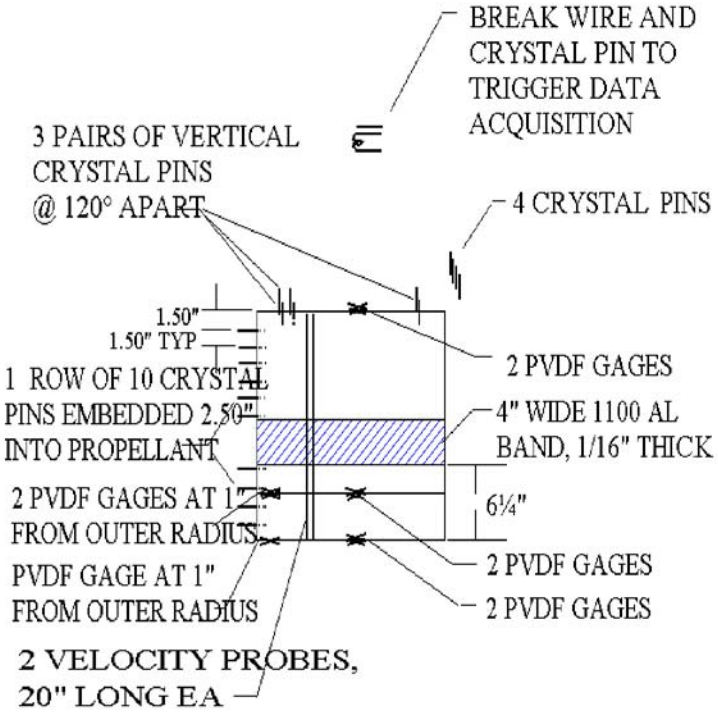

Figure 11.
Plate Two Test Sensor Positions

The 1000 and 20,000 frames per second cameras performed well in the Plate 2 experiment. Most atmospheric overpressure and crystal pin sensors provided data, but only four out of 10 OVF2 gauges gave meaningful results.Observation by video camera during the event indicated fragments of low angle flying, burning propellant fragments emerging from a dust cloud about 200 millisecs. after initiation. Infrequent pieces of unburned propellant were found on the ground ranging in size from a few grams to about 500 grams. Most unburned fragments were located in a circular pattern roughly 90 to 150 m (300 to 500 ft.) distance from ground zero. Larger fragments were much fewer than the smaller fragments. A number of aluminum oxide residue spots, perhaps, fewer than recovered unburned pieces of propellant were found on the ground in a random pattern indicating where pieces of solid propellant had fallen and burned. The steel impact plate was flat, near the center, and face down in a shallow ground crater about 15 cm (5 in.) deep and about 1.5 m (5 ft.) in diameter. This suggested that the steel plate may not have been overturned during the event. The steel plate was made thinner by the impact process since the upper side diameter was 654 mm (26.75 in.) and the lower side diameter was 622 mm (24.5 in.) versus the uniform original plate diameter of 610 mm (24 in.). The crater bottom was relatively flat with rounded corners rising to the surface, perhaps, indicating a blowing action of propellant out from under the steel plate. If this is true, the major part of the propellant energetic response to being struck by a high speed, heavy steel plate may have occurred only after the propellant with the plate on top had hit the ground. The arc of the propellant fragments observed by video supported this conclusion.

Atmospheric overpressures produced, as provided in Table 9 below by the Plate 2 test, indicated an atmospheric shock roughly equivalent to about 160 kg (580 lbs.) of TNT. Subtracting 93 kg (205 lbs.) of TNT equivalent for the combined total 290 kg (640 lbs.) of AP and 12 kg of DETA sheet driver charge, about 170 kg (375 lbs.) of TNT equivalent was produced by the propellant sample. TNT equivalents of 0.3 and 1.0 were used for the AP and DETA sheet, respectively. Using these figures, roughly 70% of the propellant sample contributed to atmospheric shock (used 1.3 TNT equivalent for propellant).

Table 9. Atmospheric Overpressures for Plate 2 Test with Low Rate Propellant

Direction	Radius m (ft.)	Arrival Time millisec	Overpressure Peak kPa (psig)
NE	46 (150)	97.1	19.0 (2.76)
SE	46 (150)	100.9	12.9 (1.87)
NE	76 (250)	178.7	8.5 (1.24)
SE	76 (250)	183.9	12.2 (1.42)
NE	107 (350)	262.3	6.4 (0.93)
SE	107 (350)	269.7	6.8 (0.99)

Table 9.
Atmospheric Overpressures for Plate 2 Test with Low Rate Propellant

Below is displayed crystal pin time of arrival data for the plate 2 test in Table 10 and PVF2 gauge data is exhibited in Table 11. Examination of these data come to the conclusion that the steel plate hit the propellant sample at about 230 m (750 ft.) per second near the edge of the propellant and faster at the center of the propellant sample. Using arrival times for crystal pin 8 (CP8) and PVF1, the plate center protruded at least 16 mm (0.6 in.) at impact between the steel plate and the propellant. Center extension may have been more since PVF2 gaauges typically lag crystal pin reaction times by a few microseconds. It is somewhat surprising that the steel plate as recovered after the Plate 2 test was rather uniformly flat. This indicates that plate bending by the acceleration process was almost exactly reversed by impact with the propellant sample. A confusing result in the crystal pin time of arrival data was the time of arrival for the plate at the propellant surface as indicated by crystal pins located between the initial steel plate position and the top of the propellant sample after the time of arrival for crystal pins inserted into the propellant cylinder. After some consultation with advisors for our program, the conclusion was that in the absense or lack of Le Croy recorder synchronization errors air shock provided by our greatly extended driver charge (1.22 m charge diameter versos 0.61 m plate diameter and 0.51 m propellant cylinder diameter) was strong enough to trigger crystal pins inserted into the propellant, but not strong enough to trigger PVF2 gauges. This suggests that the configuration of subsequent plate impact experiments will require massive shield structure around the propellant sample to prevent false readings from crystal pins embedded in the propellant. PVF2 gauge readings exhibited pressures within the impacted propellant cylinder as being between 0.8 and 9.7 kbars. Pressures were less than 40 kbars in the 22-in. critical diameter test. These low pressures in relatively strongly reacting propellant hold out hope that RTGs (radioisotope thermoelectric generators) may avoid disruption that could cause plutonium 238 dispersal in a failed launch accident using slow rate booster propellants.

Table 10. Plate 2 Impact Test Crystal Pin Data for Primary HTPB Propellant

Sensor	Distance to Propell Top mm	Delta mm	Time of Arrival microsec.	Delta	Interval Velocity mm/microsec.
1st Recorder					
CP1	-91.6	10.0	0	--	----
CP2	-81.6	10.0	49.8	49.8	0.200
CP3	-71.6	10.0	96.5	46.5	0.215
CP4	-61.6	10.0	138.3	41.8	0.239
CP5	-14.2	47.4	---	----	----
CP6	- 2.7	11.5	----	----	----
CP8	-16.3	45.3	314.8	176.5	0.257?
CP7	- 5.3	11.3	366.2	51.4	0.220
CP10	-16.7	44.9	----	-----	----
CP9	- 4.2	12.5	----	----	----
Propellant	0.0	5.3	(390.3)	(24.1)	(0.230)
2d Recorder					
Propellant	0.0	38	(349.1)	(-10.0)	(3.80)
CP11	38	----	359.1	----	?
CP12	76	38	370.3	11.2	3.39
CP13	114	38	381.9	11.6	3.27
CP14	152	38	394.4	12.5	3.04
CP15	191	38	408.7	14.3	2.66
CP16	229	38	423.1	14.4	2.64
CP17	356	127	474.2	51.1	2.49
CP18	394	38	490.5	16.3	2.33
CP19	432	38	505.7	15.2	2.50
CP20	470	38	524.6	18.9	2.01

Table 10. Plate 2 Impact Test Crystal Pin Data for Primary HTPB Propellant

Table 11. Plate 2 PVF2 Data

Sensor	Dia. to 1st AP Foil mm	Delta mm	P kbars	Time of Arrival microsec.	Delta	Interval Velocities mm/microsec.
PVF1 CT	0	0	4.0	315.2	-----	----
PVF8 CB	508	508	0.8	526.9	211.7	2.40
PVF2 CT	0	0	9.7	313.7	----	----
PVF8 CB	508	508	0.8	526.9	213.2	2.38
PVF1 CT	0	0	4.0	315.2	----	----
PVF5 EP	406	406	0.8	501.4	186.2	2.18*
PVF2 CT	0	0	9.7	313.7	----	----
PVF5 EP	406	406	0.8	501.4	187.7	2.16*

*Using a center time of arrival with an edge time of arrival may be erroneous since edge times typically lag versus the center
CT = center at top of propellant sample
CB = center at bottom of propellant cylinder
EP = 25 mm from sample perimeter between propellant pieces

Table 11. Plate 2 PVF2 Data

BOOSTER PROPELLANT MODELING

A new reactive-flow model in the CALE computer code (3) has been developed to help us understand the behavior of Titan IV propellant composed of AP, HTPB and aluminum. Such a system is characterized by two time scales which make it very difficult to use the standard Tarver Ignition-Growth-Completion (IGC) mechanism (4) to model the explosives. The first time scale is the rate of the AP-binder reaction. The second is the metal burning rate, which is slower than the AP burning rate.

In this model, we have attempted to keep the essential elements of the IGC model, while changing the meaning of some of its compontnes to more closely correlate with the mechanisms found in HTPB propellants.

Because of the disparity between the two reaction time scales, it is likely that the detonating explosive will spend a large time in a state where the AP-HTPB has all reacted, while the aluminum is mostly unreacted. Physically, the explosive goes from a material which is cold and stiff (unreacted) to a material which is warm and gassy (oxidizer and fuel reacted, aluminum not) to a material which is hot and less gassy (everything reacted). It is virtually impossible to construct the equation of state for the intermediate based on the equation of state of the reactants and products. Therefore, we found it necessary to introduce a third equation of state into the reactive flow framework. This equation of state will have the properties associated with the physical properties of reacted AP-binder products and unreacted aluminum.

Given three states that the system can travel between, it is now necessary to construct a reaction model that incorporates the reactive concepts described here.

AP + Al ---> AP products + Al ---> AP + Al products
(1)

We begin with the following assumptions:

* Three equations of state:
  A. Unreacted EoS (equation s of state)
  B. Fully reacted AP-binder, unreacted aluminum
  C. Fully reacted AP, binder and aluminum
* The aluminum only reacts with the AP-binder products.
* The AP-binder reaction is independent of the A1, except for dilution effects.
* Model the AP-binder reaction a modified Ignition and Growth terms of the IGC model.
* Model the Al reaction with a modified completion expression.

The reaction scheme can be written as follows

$$A \text{ ---> } B$$
$$B + C \text{ ---> } D$$

where A is the AP-binder reactant, B is AP-binder product, C is the aluminum, and D is the final product. The AP-binder conservation relation is

$$[A] + [B] + [D] = [E]$$

and the aluminum conservation relation is

$$[C] + [D] = [M].$$

We are using molar equivalents in these equations. equivalent of AP-binder is the amount that produces enough product gasses to react with one mole of aluminum. We now write the first reaction rate expression:

$$d[A]/dt = -k_i [A]^a I (\rho/\rho_0 - 1 - c)^n H(A - A_{i,lim}) H(\rho/\rho_0 - 1 - c)$$
$$+ -k_g [A]^{ac} ([E] - [A])^{bc} P^m \{ 1 + \varepsilon (\sigma - \sigma_0) H(\sigma - \sigma_0) H(\rho - \rho_0) \} \quad (2)$$

where k_i is the ignition rate, ρ is the current density, ρ_0 is the initial density, and c is the compression threshold for initiation. The factor $\lambda_{1\ i,lim}$ is used to cut off the ignition reaction after a few percent reaction, k_g is the reaction rate for the decomposition/burn of the AP-binder system, a_g and b_g are factors related to the geometry of the burn, and m is the pressure exponent of the burn rate. The expression σ is the effective plastic strain that the material has seen while in compression, σ_0 is the strain threshold for surface area creation, and ε is the strain-area proportionality constant.

The strain rate enhancement term in the decomposition/burn term was added after the experimental measurements indicated that there was a large second pressure pulse following the initial shock wave. The phenomenological justification for this factor is that the shear stress from the initial shock wave cracks the propellant, thereby increasing the surface area available for burning. However, while the system is in compression this new burn area only becomes available when the propellant is no longer under compression. It was decided to keep the number of coefficients in this portion of the model to a minimum because of the lack

of sufficient experimental data on the fracture of propellants to warrant a more complicated model. The aluminum reaction is written as

$$d[\mathrm{C}]/dt = -k_c\,[\mathrm{C}]^{a}_{c}\;[\mathrm{B}]^{b}_{c}\;P^{n} \tag{3}$$

where kc is the aluminum-oxidizer reaction rate, a_c and b_c are used to respectively describe geometry of the aluminum and oxidizer, and *n* is the pressure exponent of the aluminum-oxidizer burn. It is important to know the maximum extent of reaction of the system. We define the quantity D_{max} as

$$D_{max} = min\,([\mathrm{E}],\;[\mathrm{M}]). \tag{4}$$

This is the largest value of D that can be produced by these reactions. Making the substitutions:

$$1 - \lambda_1 = [\mathrm{A}]/[\mathrm{M}], \tag{5}$$

$$\lambda_2 = [\mathrm{D}]/D_{max}, \tag{6}$$

we get

$$d\lambda_1/dt = k_i\;[\mathrm{E}]^{ai-1}\;(1-\lambda_1)^{a\,i}\,(\rho/\rho_0 - 1 - c)^{\eta}\;H\,(\lambda_{1i,lim} - \lambda_1)$$

$$+\,k_g\;[\mathrm{E}]^{ag+bg-1}\;(1-\lambda_1)^{ag}\,\lambda_1^{bg}\;P^{m}\,\{1+\varepsilon(\sigma-\sigma_0)\,H\,(\sigma-\sigma_0)\,H\,(\rho_0-\rho)\} \tag{7}$$

$$d\lambda_2/dt = k_c\,D_{max}^{\,ac+bc-1}\;([\mathrm{M}]/D_{max} - \lambda_2)^{ac}\;([\mathrm{E}]\lambda_1/D_{max} - \lambda_2)^{bc}\,P^{n} \tag{8}$$

In the actual code, all of the constant prefactors are merged into one term. It is important to realize that, although there are 41 coefficients in the model, most of the coefficients are either known or easily estimated. For example, 21 coefficients are for the JWL equations of state for the reactant, intermediate, and final product. Two others define the difference in energy between the different equations of state. One determines how tight the pressure convergence should be. Another relates the relative concentrations of the components in the explosive, and should be known for any explosive. T_0 is the initial temperature of the propellant. The a and b parameters are geometric factors for the reaction rates and are determined by the mechanism for the burning of the various components. That leaves 5 ignition coefficients and the reaction prefactors, exponents, and strain enhanced burn parameters that were adjusted to model the system.

The JWL equation of state that is used for the reactant, intermediate, and product is of the form:

$$P = Ae^{-r_1 (\rho_0/\rho)} + Be^{-r_2 (\rho_0/\rho)} + C_p \omega T_p / \rho_0$$

The values used in this calculation are given in the following table:

Table 12. JWL Equation of State Parameters

Reactant		Intermediate		Product	
$\rho_{0,r}$	1.795 gm/cm^3	$\rho_{0,i}$	1.795 gm/cm^3	$\rho_{0,i}$	1.795 gm/cm^3
A_r	7.425 *Mb*	A_i	23.3483 *Mb*	A_p	1.5e9 *Mb*
B_r	-0.1751 *Mb*	B_i	-0.55051 *Mb*	B_p	0.25736 *Mb*
$r_{1,r}$	6.0	$r_{1,r}$	6.7542	$r_{1,p}$	33.296
$r_{2,r}$	2.0	$r_{2,i}$	2.27583	$r_{2,p}$	0.836225
ω_r	0.8	ω_i	0.313545	ω_p	0.658564
C_{pr}	2.22e-5 *Mb/K*	C_{pi}	7.73e-6 *Mb/K*	C_{pp}	7.47e-6 *Mb/K*
T_0	298. *K*	$Q_{r->i}$	.074 *Mb-cc/gm*	$Q_{r->p}$	.136 *Mb-cc/gm*

Table 12. JWL Equation of State Parameters

These parameters were obtained from a variety of source information. The reactant equation of state of developed by Ed Lee based on the Us - Up relation for the initial material. The intermediate equation of state was dderived from a CHEQ (5) calculation where the unreacted Al was replaced by inert carbon at the same weight percent. The release isentrope was then fit to a JWL EOS form by minimizing the error in the logarithm of the energy, after ensuring that the CJ conditions were satisfied. The final product EOS was fit in a similar manner, except that the underlying calculations were derived from a TIGER-BKW (6) calculation. The terms $Q_{r\ to\ i}$ and $Q_{i\ to\ p}$ are the amount of energy that is released going from the reactant to the intermediate, and from the intermediate to the final product. A simple strength model has been used for the propellant. It has two terms - a compressive modulus of 0.018 Mb (megabar) and a yield strength of 0.0001 Mb. The yield strength is higher than what would normally be associated with these materials. However, material strengths are known to increase at high strain rates, such as in a shock.

Unlike the equation of state parameters which are stable and are not expected to change, the reaction rate parameters have been adjusted to match experiments. It is therefore understood that these rate parameters are at best provisional. The rate parameters that were used for these calculations:

Table 13. Reactive Flow Parameters

Ignition		Growth		Completion	
$k_i [E]^{ai-1}$	1.1	$k_g [E]^{ag+bg-1}$	.1	$k_c D^{ac+bc}{}_{max}$	.01
a_i	.222	a_g	.222	a_c	.667
c	.0001	b_g	.667	b_c	1.0
η	4.	m	.8	n	.3333
$\lambda_{ii,lim}$	.04	σ_0	.1	[E]/[M]	2.26
		ε	100.0		

Table 13. Reactive Flow Parameters

The parameters used here have been designed for use in the modified version of CALE with centimeter zoning in the propellant. We used centimeter zoning because the typical zoning for explosives (mm) would have required two orders of magnitude more zones and would have also decreased the time step by an order of magnitude just due to the Courrant limit. Given both the size of the typical parts, and the length of time over which the analysis must be performed, it was decided that standard size zoning would be impractical. Thus, it is assumed that these parameters are only an approximation of their infinitesimal zoning limits.

SUMMARY

At this point in the program we are still learning the eruptive characteristics of our HTPB/AP/Al booster propellant. We have had a struggle in adapting and inventing experimental methods for elucidating the explosive traits of materials that have generally not had extended systematic investigations. We are still searching for ways to better use instrumental sensors and to get them to survive long enough to provide data that will enhance our understanding. After getting encouragement that critical diameters for 88% solids HTPB propellants might be in the range of 200 to 250 mm, we have found that the first booster propellant formulation we have looked at has a critical diameter larger than 559 mm and, perhaps, twice as large as 559 mm. Although our propellant sizes are large in normal testing of explosive materials, they are definitely subscale compared to solid propellant booster motors that can contain up to 500 metric tons of propellant. Larger size samples might be employed in the future since investigation of characteristics above critical diameter are desired. Long fabrication lead times and high costs for making samples preclude use of samples larger than we have on hand at this time. We are still looking forward to determining impact velocity thresholds for producing strong atmospheric shocks. We have obtained strong air shock yields, but rarely complete propellant consumption. We plan to gain some understanding of the change of threshold input shock intensity versus propellant grain size.

The use of a modified LLNL computer code has been rewarding. Not only did we discern a double shock explosive process in HTPB propellants, we have been able to develop a form of

the CALE code that can mimic this characteristic. This computer code involves separate reaction kinetics for the AP-binder reaction and the AP and binder products-aluminum combustion reaction. The hydrodynamic part of the CALE code can deal with different equations of state involved with a variety of colliding surfaces that might occur in a failed space booster launch operation. This is a great aid in reducing the number of needed experiments. With the computer code we hope to meet our present goals without resorting to greatly different propellant sample size tests.

Solid rocket booster propellant in explosive events seems to provide high atmospheric overpressure yields without being involved in true detonations. If detonations are steady state supersonic events in the energetic material and deflagrations are explosive events characterized by subsonic shock in the energetic materials, perhaps, a new definition for an explosive process may need to be defined. This process involves a supersonic, slowing, long propagating shock through an energetic material. Such a process might be called a dying detonation, and would not have the brisance and cratering capability exhibited by normal detonating substances. None of our experiments with the slow rate HTPB propellant have as yet yielded complete energetic yield to atmospheric shock as some measure of burning propellant fragments have been observed visually, by physical recovery of unburned propellant pieces, and by *burn* spots of aluminum oxide residue on the ground. This cannot be said for the higher burn rate propellant that contained iron oxide. The difference in shock speeds for the two propellants is only on the order of 0.8 mm per microsecond. This difference seems to make a great difference in capability to form ground craters and to produce evidence of burning and unburned propellant fragments. Although the compositions of the two propellants are similar, the differences causing the change in explosive character are unknown. Further effort will proceed in trying to understand the strange nature of these HTPB rocket booster propellants.

REFERENCES

(1) Brunet, J. and Salvetat, B., "Detonation Critical Diameter of Advanced Solid Rocket Propellants," presented at the Joint International Symposium on Compatibility of Plastics and Other Materials with Explosives, Propellants, Pyrotechnics and Processing of Explosives, Propellant and Ingredients, New Orleans, Louisiana, 18-20 April 1988.

(2) Merrill, C.I., "Large Class 1.3 Rocket Motor Detonation Behavior," in Proceedings of the 1992 Department of Defense Explosive Safety Board Meeting, Sep 1992.

(3) R. Tipton, "CALE User's Manual", Lawrence Livermore National Laboratory, Livermore, CA.

(4) C.M. Tarver, J.O. Hallquist, L.M. Erickson,"Modeling short pulse duration shock initiation of solid explosives", 8th Detonation Symposium, pp. 951-961, 1985.

(5) A.L. Nichols and F.H. Ree, "CHEQ 2.0 User's Manual" UCRL-MA 106754, Lawrence Livermore National Laboratory, Livermore, CA, December 1990.

(6) M. Cowperthwaite and W.H. Zwisler, "Tiger Computer Program Documentation", SRI Publication No. Zi06, 1973.

ACKNOWLEGEMENTS

We thank the Titan IV System Program Office, the Research Triangle Institute of Cocoa Beach, the Eastern Range Safety Office at Patrick AFB, and our project consultants for financial support and encouragement without which this experimental and code developing program would not have been possible.

We owe many thanks to Wyle laboratories personnel for timely completion of the many nonstandard tasks that have been given to them for this project. Special mention to Ron Lambert, test engineer, for innovative and practical test designs; Ted Mullins, Wyle supervisor for innovative construction, purchasing, and finding the noiseless trunkline; Larry Wilburn and John Morrow, mechanics, who have provided innovative test article support construction; Ray Gonzales and Ray Miskofsky, instrumentation engineers; and the many others supporting the effort who have not been mentioned.